# Vibrational relaxation of $CH_3I$ in the gas phase and in solution

Christopher G. Elles, M. Jocelyn Cox, and F. Fleming Crim[a)]
*Department of Chemistry, University of Wisconsin-Madison, Madison, Wisconsin 53706*

(Received 28 October 2003; accepted 22 January 2004)

Transient electronic absorption measurements reveal the vibrational relaxation dynamics of $CH_3I$ following excitation of the C–H stretch overtone in the gas phase and in liquid solutions. The isolated molecule relaxes through two stages of intramolecular vibrational relaxation (IVR), a fast component that occurs in a few picoseconds and a slow component that takes place in about 400 ps. In contrast, a single 5–7 ps component of IVR precedes intermolecular energy transfer (IET) to the solvent, which dissipates energy from the molecule in 50 ps, 44 ps, and 16 ps for 1 M solutions of $CH_3I$ in $CCl_4$, $CDCl_3$, and $(CD_3)_2CO$, respectively. The vibrational state structure suggests a model for the relaxation dynamics in which a fast component of IVR populates the states that are most strongly coupled to the initially excited C–H stretch overtone, regardless of the environment, and the remaining, weakly coupled states result in a secondary relaxation only in the absence of IET.
 [DOI: 10.1063/1.1676292]

## I. INTRODUCTION

The flow of vibrational energy plays a central role in chemical reaction dynamics. Intramolecular vibrational relaxation (IVR) moves energy within an excited molecule and intermolecular energy transfer (IET) dissipates excess energy to the solvent. These processes, which collectively we call vibrational relaxation, govern the evolution of the vibrational energy distribution, thus influencing the rate, yield, and, in favorable cases, the outcome of vibrationally activated reactions.[1] Although many studies examine vibrational relaxation in either the gas phase[2–5] or in solution,[6–8] only a few experiments directly compare the relaxation dynamics for the isolated and solvated molecule using the same technique.[9–17] In this paper we examine the influence that solvation has on IVR and IET by comparing the vibrational relaxation of $CH_3I$ in various solvents and in the isolated molecule.

Theoretical treatments of energy transfer provide some insight into the influence of solvation on vibrational relaxation. One approach is the isolated binary collision (IBC) model, which assumes that energy transfer is proportional to the solvent–solute collision rate.[6,18,19] This simple picture is limited, however, because the definition of a two-body collision is ambiguous in solution, where the solute continuously interacts with its surroundings. The IBC model also cannot describe IVR in an isolated molecule. Time-dependent perturbation theory provides a more explicit description of vibrational relaxation. State-specific treatment of the relaxation accounts for both energy transfer to the solvent and solvent-mediated state-to-state energy transfer within the molecule, where low frequency solvent modes make up the energy difference between vibrational states of the excited molecule.[7,20–23] These theoretical results indicate that solvation plays an important role in both IVR and IET.

Experimental studies of gas phase IVR often use high-resolution spectroscopy to measure the energies, intensities, and linewidths of transitions to the molecular eigenstates. This spectroscopic information reveals the anharmonic couplings among zero-order basis states (such as the normal modes) that are responsible for energy flow in the isolated molecule.[2–5] Line broadening frequently makes linear spectroscopy impractical in solution, however, and time-domain methods are generally a better approach.[8,24] Pump–probe experiments directly observe energy flow within and out of a molecule by exciting a nonstationary vibrational state with one laser pulse and then probing the evolution of the system as a function of time with a second pulse.[25,26] Infrared absorption,[27–32] anti-Stokes Raman scattering,[33–37] and ultraviolet absorption[38–49] are the most common methods for probing the vibrational dynamics in the ground electronic state and are generally most useful in the condensed phase where it is possible to obtain a high density of vibrationally excited molecules. In fact, there are relatively few time-resolved studies of IVR in the ground electronic state for gas phase systems.

Studies examining the solvent influence on vibrational relaxation often rely on changing the nature of the solvent. Systematically exploring different solvent properties, such as polarity and polarizability, shows which traits have the largest impact on vibrational relaxation. Several of these studies provide evidence of solvent-assisted IVR since the relaxation rate changes with the solvent.[27–29,40–42] Another approach is to monitor vibrational relaxation in small clusters, where ''solvent'' molecules form van der Waals bonds to the molecule of interest. The presence of only a few ''solvent'' molecules can dramatically affect the relaxation dynamics by introducing low frequency intermolecular modes that influence IVR and facilitate IET.[50–55] Similarly, supercritical fluids make it possible to change the solvent density from gas-like to liquidlike.[48,49,56–59] The IBC model successfully predicts the general trend that both the IVR and IET rates increase with increasing solvent density, but intramolecular relaxation occurs even in the absence of solvent. Thus, the isolated molecule is an important reference point. Compari-

a)Electronic mail: fcrim@chem.wisc.edu

 

son of the IVR rate in supercritical fluid solvents to the gas phase rate by Fayer and co-workers,[9–12] who examine $W(CO)_6$, and by von Benten *et al.*,[13] who study benzene, reveals the extent of the solvent influence in these systems. In addition to the supercritical fluid experiments, Yoo *et al.*[15–17] directly compare IVR in both the room temperature gas and in liquid solutions for various acetylenic molecules. Here we study the vibrational dynamics of $CH_3I$ in the gas phase and in solution.

## II. EXPERIMENT

We use transient electronic absorption[39] to monitor the vibrational dynamics of $CH_3I$ following excitation of the C–H stretch overtone in the gas phase and in solution. An infrared pump pulse vibrationally excites the molecule, and we monitor the change in absorption of an ultraviolet probe pulse as a function of the delay between pulses. The absorption increases on the long wavelength edge of the electronic transition as energy flows from the initially excited state into the (Franck–Condon active) C–I stretching mode.[60,61] The experiment probes excitation in vibrational modes that become populated only *after* energy flows out of the initially excited state, providing a measure of the IVR time. In the presence of solvent, intermolecular energy transfer to the surroundings lowers the total energy of the $CH_3I$ molecule, allowing observation of the flow of energy out of the molecule as well.

The infrared pump and ultraviolet probe pulses come from nonlinear frequency conversion of the light from a regeneratively amplified Ti:sapphire laser (Clark MXR, CPA-1000), which initially produces 1 mJ, 100 fs pulses centered at 800 nm at a repetition rate of 1 kHz. An optical parametric amplifier (OPA) converts approximately 50% of the light from the Ti:sapphire laser into 30 $\mu$J of 1.7 $\mu$m (6000 $cm^{-1}$) light for the excitation pulse. Two successive type I BBO crystals frequency quadruple the output from a second OPA, pumped with 30% of the Ti:sapphire light, to provide probe pulses that are tunable down to 290 nm. For the experiments in solution, a gold-coated parabolic mirror ($f=100$ mm) focuses the pump beam to a diameter of 100 $\mu$m, and a 120 mm lens focuses the probe beam to a similar size. We circulate 1 M solutions of $CH_3I$ in $CCl_4$, $CDCl_3$, or $(CD_3)_2CO$ through a slit nozzle to form a 250 $\mu$m thick liquid jet in which the laser beams intersect each other at a small angle. For the gas phase experiments, 300 mm and 400 mm lenses focus the infrared and ultraviolet beams, respectively, and a dichroic mirror collinearly overlaps and directs them through a 40 mm stainless steel cell with 2 mm thick quartz windows. Evacuating the cell and filling it with the vapor pressure from a reservoir of liquid $CH_3I$ at ambient temperature yields pressures up to 350 Torr, which we continuously monitor with a capacitance manometer (MKS, Baratron). The average focal diameter of the pump beam in the cell is about 250 $\mu$m, and the probe beam is slightly smaller. A Fresnel rhomb sets the relative polarization of the pump and probe beams to the magic angle (54.7°) in order to eliminate rotational contributions to the signal.

Silicon photodiodes measure the probe intensity before and after the sample to account for fluctuations in the laser intensity, and an optical chopper blocks every other pump pulse for active background subtraction. We use a computer controlled translation stage (Aerotech, Unidex 100) to vary the relative delay between pump and probe pulses by as much as 1.3 ns, corresponding to a translation of almost 20 cm. Averaging between 1000 and 5000 laser shots per point gives a noise level of about 0.01 m OD, although the gas phase traces are not reproducible with the same precision. We use $CH_3I$ (Aldrich), $CCl_4$ (Aldrich), $CDCl_3$ (Cambridge Isotope Labs), and $(CD_3)_2CO$ (Cambridge Isotope Labs) without further purification.

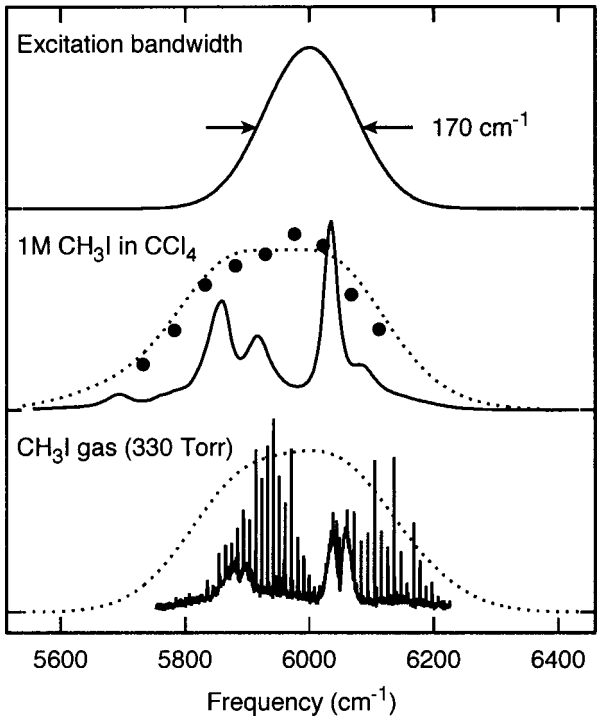


FIG. 1. Vibrational spectra of 1 M $CH_3I$ in $CCl_4$ (middle) and $CH_3I$ gas (bottom) in the region of the C–H stretch overtone. Dotted lines are a convolution of the absorption spectra with a 170 $cm^{-1}$ Gaussian corresponding to the excitation laser bandwidth (top trace), and the closed circles are the measured absorption of the excitation laser pulses in a 1 cm cell of 1 M $CH_3I$ in $CCl_4$ (maximum absorbance of 0.34).

## III. RESULTS AND ANALYSIS

Figure 1 shows infrared spectra of $CH_3I$ in the region of the C–H stretch overtone for a 1 M solution in $CCl_4$ (middle trace) and for the gas at 330 Torr (bottom trace). The conventional absorption spectrum of the solution has 3.5 $cm^{-1}$ resolution, and the gas phase photoacoustic spectrum has a resolution of 0.05 $cm^{-1}$. We obtain the photoacoustic spectrum by passing narrow bandwidth infrared light through a cell containing $CH_3I$ gas and measuring the photoacoustic response with a microphone.[62] For comparison, we convolute the solution and gas phase spectra with a 170 $cm^{-1}$ Gaussian function (top trace), corresponding to the bandwidth of the ultrafast laser pulse, to obtain the dotted lines in Fig. 1. Also shown is the absorption spectrum that we measure for the 1 M $CH_3I$ solution in a 1 cm cell by tuning the infrared wavelength of the short-pulse OPA (closed circles).

### A. Vibrational relaxation in solution

Figure 2 shows the transient electronic absorption of $CH_3I$ in the various solvents following excitation of the first overtone of the C–H stretch. As in our previous work,[39–42] we assign the rise and decay of the signal to IVR and IET, respectively. The signal rises as vibrational energy flows from the initially excited C–H stretch overtone into states that contain C–I stretching character and then decays as energy dissipates into solution. In this sequential two step process,

$$CH_3I(v_{C-H}=2) \xrightarrow{\text{IVR}} CH_3I(v_{C-I}=n) \xrightarrow{\text{IET}} CH_3I(v=0), \tag{1}$$

the Franck–Condon active C–I stretch mode contains an average of $n$ quanta of excitation at intermediate times.

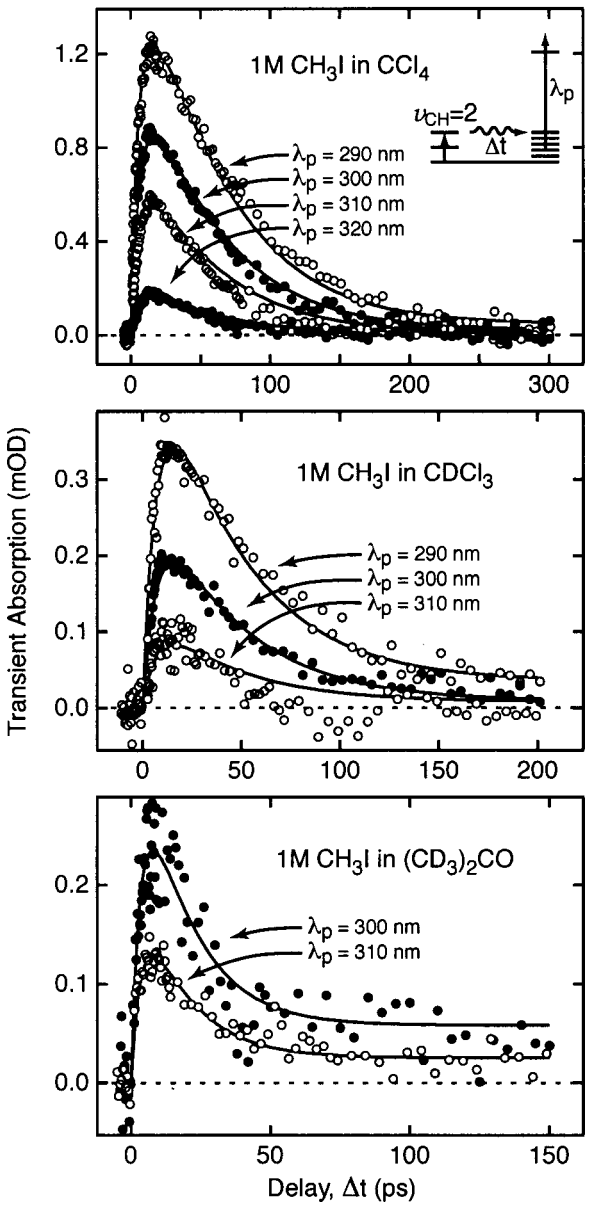


FIG. 2. Transient electronic absorption of $CH_3I$ in $CCl_4$, $CDCl_3$, and $(CD_3)_2CO$ at various probe wavelengths, $\lambda_p$. The fit to the data in each solvent uses the temperature-dependent absorption model to obtain the IVR and IET times, $\tau_{IVR}$ and $\tau_{IET}$, listed in Table I.

Fitting the data for each probe wavelength to the sum of a rising exponential and a decaying exponential gives a decay time that becomes as much as a factor of 2 longer with decreasing probe wavelength. As our previous experiments show,[39,42] this probe wavelength dependence arises from a predominantly statistical IVR mechanism, and we model the energy transfer dynamics as the rise and fall of a phenomenological vibrational temperature. Measuring the temperature dependence of the long wavelength edge of the $CH_3I$ electronic absorption spectrum in $CCl_4$ between 273 K and 312 K and extrapolating to higher temperatures allows us to fit the data at all probe wavelengths simultaneously in order to extract one IVR time and one IET time for each solvent. The resulting fits, shown in Fig. 2, yield IVR and IET times of $\tau_{IVR}=7\pm1$ ps and $\tau_{IET}=50\pm5$ ps for $CH_3I$ in $CCl_4$, $\tau_{IVR}=7\pm2$ ps and $\tau_{IET}=44\pm8$ ps in $CDCl_3$, and $\tau_{IVR}=5\pm3$ ps and $\tau_{IET}=16\pm6$ ps in $(CD_3)_2CO$.[63] Low signal intensity and a narrow range of probe wavelengths contribute to the relatively large uncertainty in the fit for the acetone solution. Table I summarizes the vibrational relaxation times in the various solvents.

### B. Vibrational relaxation in the gas phase

The transient electronic absorption of $CH_3I$ behaves quite differently following excitation of the C–H stretch overtone in the gas phase, as shown in Fig. 3. The signal rises on two distinct time scales, which we model as successive steps of intramolecular vibrational relaxation,

TABLE I. Intramolecular vibrational relaxation (IVR) and intermolecular energy transfer (IET) times for $CH_3I$ in various solvents and in the gas phase.

| Solvent | $\tau_{IVR}$ (fast)/ps | $\tau_{IVR}$ (slow)/ps | $\tau_{IET}$/ps |
|---|---|---|---|
| $CCl_4$ | 7±1 | ··· | 50±5 |
| $CDCl_3$ | 7±2 | ··· | 44±8 |
| $(CD_3)_2CO$ | 5±3 | ··· | 16±6 |
| Gas phase | <7[a] | 400±200 | ··· |

[a]The fast risetime of the gas phase signal increases with probe wavelength from 2±1 ps to 7±3 ps, see Fig. 4.

$$CH_3I(v_{C-H}=2) \xrightarrow{\text{IVR(fast)}} CH_3I(v_{C-I}=n) \xrightarrow{\text{IVR(slow)}} CH_3I(v_{C-I}=m). \quad (2)$$

In the absence of collisional relaxation, all of the vibrational energy remains in the initially excited $CH_3I$ molecule. Also, because the signal rises in both steps, the level of vibrational excitation in the C–I stretch coordinate must increase during each stage of IVR. The average number of quanta of C–I stretch increases to $n$ during the fast component of IVR and then to $m$ during the slow component ($n<m$). Fits of the gas phase data to the sum of two rising exponentials (solid lines in Fig. 3) reveal that the fast rise takes a few picoseconds and that the slow rise occurs over about 400 ps. The average contribution of the fast rise to the total signal amplitude is $32\pm5\%$, independent of the probe wavelength and sample pressure.

The closed circles in Fig. 4 show the probe wavelength dependence of the gas phase rise times, $\tau_{fast}$ and $\tau_{slow}$, where the uncertainties are the deviation among the fits to several traces. (For comparison with the fast rise in the gas phase, the open circles in the top panel are the exponential risetimes of $CH_3I$ in $CCl_4$ solution.) The uncertainty in the slow gas phase rise is particularly large because the experiment is extremely sensitive to laser beam overlap in the gas cell. Even very small fluctuations in the direction or divergence of the laser beams significantly change the signal amplitude, and the relatively large range of motion on the optical delay stage amplifies the effect of these deviations. Consequently, reproducing the signal over the entire range of delay times is difficult, and we are unable to apply a temperature dependent absorption model similar to the one that we use for the solution data.

Figure 4 shows that the initial rise in the gas phase signal is faster for shorter probe wavelengths and that the risetime of the second component is constant within the experimental uncertainty. The fast rise has a time scale and a probe wavelength dependence that are comparable to those in solution. In contrast, the slow rise has no analogous component because energy transfer to the solvent relaxes the molecule on a faster time scale. Collisional relaxation does not appear to contribute to the slow signal in the gas phase experiment, even though the average time between collisions is about 500 ps at 350 Torr. The slow risetime is roughly the same for $CH_3I$ pressures between 350 Torr and 50 Torr, and extrapolating the relaxation rate to the limit of zero pressure, even using the steepest slope that our relatively large error bars allow, suggests that the slow component of IVR persists *even in the absence of collisions*.

Another possible origin of the gas phase signal, which we also discount, is that vibrational predissociation of $CH_3I$ dimers produces the rise in the transient absorption signal. Waschewsky *et al.*[64] infer that a large fraction (44%–77%) of $CH_3I$ is in the form of dimers at the temperature and pressure of our experiment. In addition, molecular beam data show that the electronic spectrum of the monomer lies at lower energy than that of the dimer,[65,66] potentially leading to an increase in transient absorption upon dissociation of the dimer. If the fast component of the signal were due to dimer dissociation, however, the risetime would not depend on the probe wavelength because the whole spectrum would shift

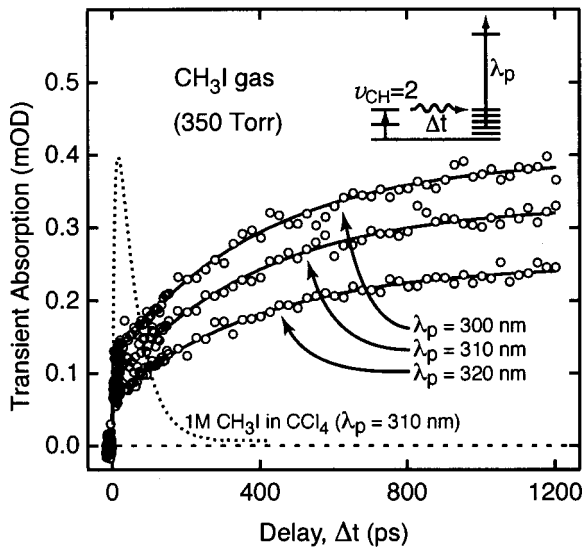


FIG. 3. Transient electronic absorption of $CH_3I$ gas at 350 Torr for various probe wavelengths, $\lambda_p$. Each trace is fit to the sum of two rising exponentials, with time constants $\tau_{fast}$ and $\tau_{slow}$, and the dotted line shows the transient absorption in solution.

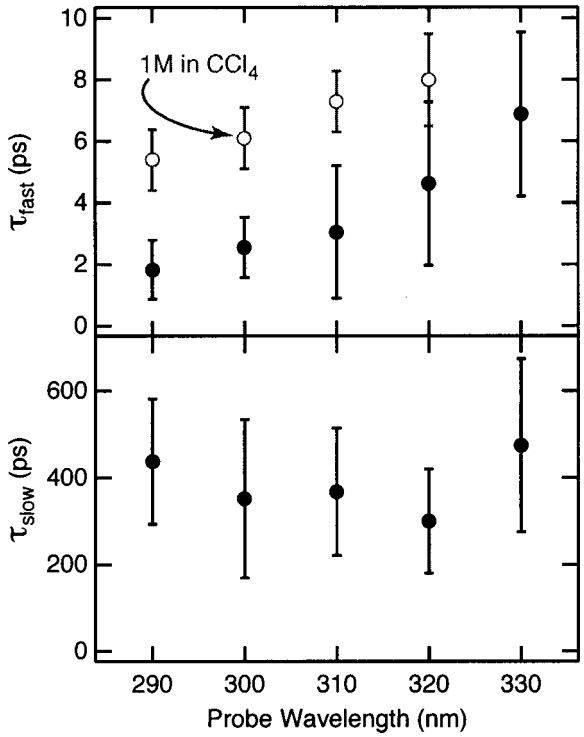


FIG. 4. Probe wavelength dependence of the fast (top) and slow (bottom) signal risetimes in the gas phase. Risetimes for $CH_3I$ in $CCl_4$ are shown in the top panel for comparison.

with the single time constant of the dissociation. If the fast component were instead due to IVR, then the initial redistribution of energy would dissociate the dimer and there would not be a slow dissociation.[67] We also find that varying the pressure between 350 Torr and about 50 Torr of $CH_3I$ and the temperature between 293 K and 370 K, each of which would reduce the dimer fraction,[68] produces no noticeable change in the risetimes or the *relative* amplitudes of the fast and slow components. Furthermore, the photoacoustic spectrum in the C–H stretch overtone region is identical at $<3$ Torr and at 330 Torr, indicating that any dimers that are present do not have an appreciable infrared absorption in this region compared to the monomers. We conclude that dissociation of $CH_3I$ dimers does not contribute to our transient electronic absorption signal and that both components of the gas phase signal arise from purely *intra*molecular vibrational relaxation.

## IV. DISCUSSION

Comparing the vibrational dynamics in the gas phase and in solution shows that the environment strongly influences the relaxation of $CH_3I$ following excitation of the C–H stretch overtone. In solution, *intra*molecular vibrational relaxation and *inter*molecular energy transfer to the solvent cause a rise and subsequent decay of the signal, but the two distinct components of IVR in the gas phase cause the signal to rise on two time scales. The most apparent difference is the dissipation of vibrational energy from the solvated molecule on a time scale that is faster than the second, slow component of IVR in the gas phase. This observation suggests that vibrational energy only partially equilibrates within the solvated molecule before dissipating into the surroundings. In contrast, the comparable time scale and wavelength dependence of the rise in solution and the fast component in the gas phase suggest that they result from similar IVR processes. Examining the vibrational state structure in the region of the C–H stretch overtone helps explain this behavior.

The state structure is a key element of IVR because the number of states that accept energy from the initially excited state, along with the relative energy separation and coupling strengths, govern the relaxation. It is useful to relate the vibrational states of a molecule to the relaxation dynamics using a tier model, which organizes the states according to the strength of their coupling to the initially excited state.[2–4] The most strongly coupled states compose the first tier and play a dominant role in the initial relaxation because the rate of energy transfer depends on coupling strength. Conversely, the more weakly coupled states constitute higher tiers and contribute to the relaxation on longer time scales, depending on their number and relative coupling strength. One approximate method for assessing the relative coupling strengths is to enumerate the states as a function of their order of coupling to the initially excited state.[40–42,69–71] The coupling order is the number of quanta exchanged in making a transition between states. For a small molecule, such as $CH_3I$, the coupling strength decreases more rapidly with coupling order than the number of states increases. The top panel of Fig. 5 shows all of the states that lie within 500 $cm^{-1}$ of the initially excited C–H stretch overtone arranged by coupling order. The states come from a harmonic state count using the vibrational frequencies in Table II,[72] and we separate degenerate states by 10 $cm^{-1}$ to show the number of states more clearly. The lower panel of Fig. 5 shows the total density of vibrational states (open bars) and the density of states containing C–I stretch excitation (closed bars), in the region of the C–H stretch overtone, for each order of coupling. The latter states are important because population of these states increases the transient electronic absorption.

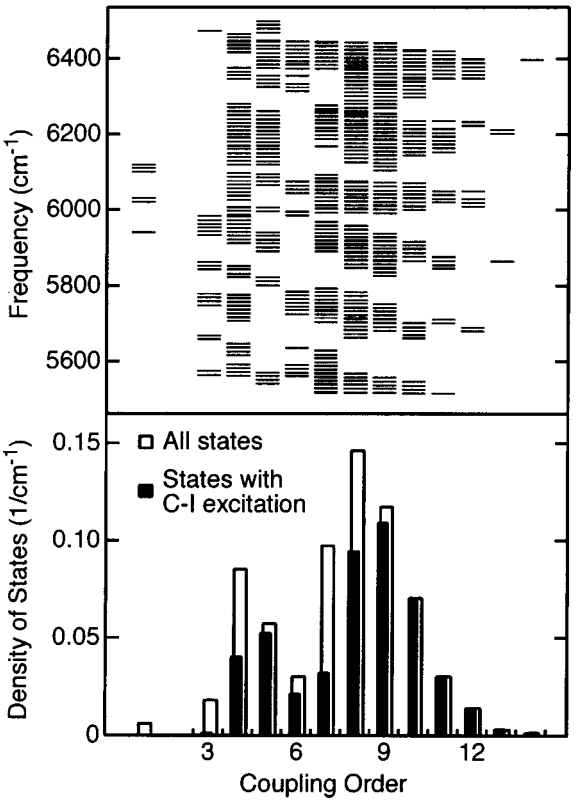


FIG. 5. States within 500 $cm^{-1}$ of the C–H stretch overtone (top) and the corresponding densities of states (bottom) as a function of the coupling order. States containing excitation in the C–I stretch mode contribute to the transient absorption signal.

A striking feature of Fig. 5 is the bimodal distribution of states as a function of the coupling order. In fact, this state structure explains the IVR that we observe. The initially excited C–H stretch overtone quickly relaxes into the relatively strongly coupled states, those with a coupling order of three to six, and the remaining, more weakly coupled states participate on a longer time scale. Both components of IVR are

TABLE II. Vibrational normal mode frequencies and symmetries for $CH_3I$.[a]

| Mode | Motion | Energy/$cm^{-1}$ | Symmetry |
|---|---|---|---|
| $\nu_1$ | $CH_3$ sym. stretch | 2970 | $a_1$ |
| $\nu_2$ | $CH_3$ sym. def. | 1252 | $a_1$ |
| $\nu_3$ | CI stretch | 533 | $a_1$ |
| $\nu_4$ | $CH_3$ deg. stretch | 3060 | $e$ |
| $\nu_5$ | $CH_3$ deg. def. | 1436 | $e$ |
| $\nu_6$ | $CH_3$ deg. rock | 882 | $e$ |

[a]Reference 72.

evident in the isolated molecule, but energy transfer to the solvent is more efficient than the slower IVR process in solution and only a single, fast component of IVR survives. As the bottom panel of Fig. 5 shows, most of the states in the molecule involve at least some degree of excitation in the Franck–Condon active (C–I stretch) mode and therefore contribute to an increase in the transient absorption. Additionally, states with higher coupling order typically contain more quanta of the low frequency C–I stretch, accounting for the signal increase during *both* stages of gas phase IVR.

Our observations are consistent with other recent time-resolved vibrational relaxation experiments. For example, an extensive treatment of the relaxation following excitation of the fundamental C–H stretch in a series of acetylenic molecules by Yoo *et al.*[15–17] shows that some of the molecules have two intramolecular relaxation times in the gas phase although only the fast component survives in solution. They also determine that the fast relaxation comes from strong coupling between the initially excited C–H stretch and a sparse set of states containing two quanta of C–H bend and that the slow relaxation results from weak coupling of these states to the remaining states. In another experiment, von Benten *et al.*[13] observe two IVR times following excitation of two quanta of C–H stretch for benzene in the gas phase and in supercritical $CO_2$. Both components of IVR survive in the supercritical fluid, but solvation has a much stronger influence on the slow component than on the fast one.

Only one component of IVR occurs for $CH_3I$ in solution, in contrast to the two time scales that we observe in the isolated molecule. The rise in solution and the fast component in the gas phase are the result of a similar IVR process since the same states contribute to the relaxation in each case, but the IVR in solution is slightly *slower* than the fast component of IVR in the gas phase (as shown in the top panel of Fig. 4). It seems surprising that IVR occurs more slowly in solution because in the simplest picture one expects the solvent to accelerate IVR by making up the energy gap between states within the molecule. The slower relaxation in solution probably results from vibrational frequencies shifting by different amounts upon solvation, which changes the energy gap between states and leads to the different relaxation times. It is unclear if the change is due primarily to a static shift or a dynamical process that increases the *average* energy gap between states. In any case, at least one component of the internal relaxation occurs on a similar time scale in the gas phase and in solution.

We also examine the influence of the solvent identity on IVR and IET, since solvent–solute interactions can affect the vibrational relaxation (Table I). Changing the solvent has only a weak influence on the IVR time for $CH_3I$, but the trend is qualitatively similar to our previous experiments for $CH_2I_2$, where acetone and benzene accelerate IVR relative to the more weakly interacting solvents, $CCl_4$ and $CDCl_3$.[39–42] The weaker solvent dependence in $CH_3I$ is not surprising because the faster 5–7 ps relaxation that we observe limits the extent to which the solvent accelerates IVR compared to that in $CH_2I_2$. The IET rate depends more strongly on the identity of the solvent than the IVR rate since solvent–solute interactions directly transfer energy between molecules, and we find that acetone clearly accelerates IET for $CH_3I$ relative to the more weakly interacting $CCl_4$ and $CDCl_3$. In all of the solvents, however, intermolecular energy transfer to the surroundings occurs on a faster time scale than the slow component of IVR, which only appears in the gas phase.

## V. SUMMARY

We use transient electronic absorption to monitor the flow of vibrational energy in both isolated and solvated $CH_3I$ following excitation of the C–H stretch overtone. In solution, the electronic absorption rises and decays, corresponding to *intra*molecular vibrational relaxation within the molecule and *inter*molecular energy transfer to the solvent, respectively. Using a temperature dependent absorption model to account for the probe wavelength dependence, we determine an IVR time of 5–7 ps and an IET time of 50 ps or less, depending on the solvent. The transient absorption for the isolated molecule, in contrast, has a fast initial increase that is complete within a few picoseconds followed by a slow increase of about 400 ps, the result of two distinct components of IVR. Strong coupling between the initially excited C–H stretch overtone and states coupled up to sixth order lead to the intramolecular relaxation in solution and the fast initial relaxation in the gas phase. Relaxation into the remaining, more weakly coupled states causes the slow component of IVR in the gas phase, but intermolecular energy transfer to the solvent dissipates energy from the molecule before these states become populated in solution.

## ACKNOWLEDGMENTS

We thank Robert J. Holiday and J. Matthew Hutchison for assistance obtaining photoacoustic spectra, and Professor Brooks H. Pate and Professor Bernd Abel for sharing their results prior to publication. This research is supported by the Air Force Office of Scientific Research.

[1] F. F. Crim, J. Phys. Chem. **100**, 12725 (1996).
[2] P. R. Stannard and W. M. Gelbart, J. Phys. Chem. **85**, 3592 (1981).
[3] K. K. Lehmann, G. Scoles, and B. H. Pate, Annu. Rev. Phys. Chem. **45**, 241 (1994).
[4] D. J. Nesbitt and R. W. Field, J. Phys. Chem. **100**, 12735 (1996).
[5] M. Quack, Annu. Rev. Phys. Chem. **41**, 839 (1990).
[6] D. W. Oxtoby, Adv. Chem. Phys. **47**, 487 (1981).
[7] J. C. Owrutsky, D. Raftery, and R. M. Hochstrasser, Annu. Rev. Phys. Chem. **45**, 519 (1994).
[8] R. M. Stratt and M. Maroncelli, J. Phys. Chem. **100**, 12981 (1996).
[9] D. J. Myers, M. Shigeiwa, M. D. Fayer, and R. Silbey, Chem. Phys. Lett. **312**, 399 (1999).
[10] D. J. Myers, M. Shigeiwa, M. D. Fayer, and B. J. Cherayil, Chem. Phys. Lett. **313**, 592 (1999).
[11] D. J. Myers, M. Shigeiwa, M. D. Fayer, and B. J. Cherayil, J. Phys. Chem. B **104**, 2402 (2000).
[12] C. Stromberg, D. J. Myers, and M. D. Fayer, J. Chem. Phys. **116**, 3540 (2002).
[13] R. von Benten, A. Charvat, O. Link, and B. Abel, Chem. Phys. Lett. (to be published).
[14] R. von Benten, O. Link, B. Abel, and D. Schwarzer, J. Phys. Chem. A **108**, 363 (2004).
[15] H. S. Yoo, M. J. DeWitt, and B. H. Pate, J. Phys. Chem. A **108**, 1348 (2004).
[16] H. S. Yoo, M. J. DeWitt, and B. H. Pate, J. Phys. Chem. A **108**, 1365 (2004).

[17] H. S. Yoo, M. J. DeWitt, and B. H. Pate, J. Phys. Chem. A **108**, 1380 (2004).
[18] D. J. Russell, M. E. Paige, and C. B. Harris, Ber. Bunsenges. Phys. Chem. **95**, 299 (1991).
[19] D. J. Russell and C. B. Harris, Chem. Phys. **183**, 325 (1994).
[20] S. Velsko and D. W. Oxtoby, J. Chem. Phys. **72**, 2260 (1980).
[21] V. M. Kenkre, A. Tokmakoff, and M. D. Fayer, J. Chem. Phys. **101**, 10618 (1994).
[22] S. A. Egorov and J. L. Skinner, J. Chem. Phys. **105**, 7047 (1996).
[23] S. A. Egorov and J. L. Skinner, J. Chem. Phys. **112**, 275 (2000).
[24] Y. Q. Deng and R. M. Stratt, J. Chem. Phys. **117**, 1735 (2002).
[25] A. Seilmeier and W. Kaiser, in *Ultrashort Laser Pulses*, edited by W. Kaiser (Springer-Verlag, Berlin, 1988), Vol. 60, p. 279.
[26] T. Elsaesser and W. Kaiser, Annu. Rev. Phys. Chem. **42**, 83 (1991).
[27] H. J. Bakker, P. C. M. Planken, and A. Lagendijk, Nature (London) **347**, 745 (1990).
[28] H. J. Bakker, P. C. M. Planken, and A. Lagendijk, J. Chem. Phys. **94**, 6007 (1991).
[29] H. J. Bakker, J. Chem. Phys. **98**, 8496 (1993).
[30] W. T. Grubbs, T. P. Dougherty, and E. J. Heilweil, Chem. Phys. Lett. **227**, 480 (1994).
[31] A. Tokmakoff, B. Sauter, and M. D. Fayer, J. Chem. Phys. **100**, 9035 (1994).
[32] G. Seifert, R. Zurl, T. Patzlaff, and H. Graener, J. Chem. Phys. **112**, 6349 (2000).
[33] K. Spanner, A. Laubereau, and W. Kaiser, Chem. Phys. Lett. **44**, 88 (1976).
[34] H. Graener and A. Laubereau, Appl. Phys. B: Photophys. Laser Chem. **29**, 213 (1982).
[35] J. C. Deak, L. K. Iwaki, and D. D. Dlott, J. Phys. Chem. A **102**, 8193 (1998).
[36] L. K. Iwaki and D. D. Dlott, J. Phys. Chem. A **104**, 9101 (2000).
[37] Z. H. Wang, A. Pakoulev, and D. D. Dlott, Science **296**, 2201 (2002).
[38] N. H. Gottfried, A. Seilmeier, and W. Kaiser, Chem. Phys. Lett. **111**, 326 (1984).
[39] D. Bingemann, A. M. King, and F. F. Crim, J. Chem. Phys. **113**, 5018 (2000).
[40] C. M. Cheatum, M. M. Heckscher, D. Bingemann, and F. F. Crim, J. Chem. Phys. **115**, 7086 (2001).
[41] M. M. Heckscher, L. Sheps, D. Bingemann, and F. F. Crim, J. Chem. Phys. **117**, 8917 (2002).
[42] C. G. Elles, D. Bingemann, M. M. Heckscher, and F. F. Crim, J. Chem. Phys. **118**, 5587 (2003).
[43] A. Charvat, J. Assmann, B. Abel, and D. Schwarzer, J. Phys. Chem. A **105**, 5071 (2001).
[44] A. Charvat, J. Assmann, B. Abel, D. Schwarzer, K. Henning, K. Luther, and J. Troe, Phys. Chem. Chem. Phys. **3**, 2230 (2001).
[45] J. Assmann, A. Charvat, D. Schwarzer, C. Kappel, K. Luther, and B. Abel, J. Phys. Chem. A **106**, 5197 (2002).
[46] J. Assmann, R. von Benten, A. Charvat, and B. Abel, J. Phys. Chem. A **107**, 5291 (2003).
[47] D. Schwarzer, C. Hanisch, P. Kutne, and J. Troe, J. Phys. Chem. A **106**, 8019 (2002).
[48] K. Sekiguchi, A. Shimojima, and O. Kajimoto, Chem. Phys. Lett. **356**, 84 (2002).
[49] K. Sekiguchi, A. Shimojima, and O. Kajimoto, Chem. Phys. Lett. **370**, 303 (2003).
[50] T. Kobayashi and O. Kajimoto, J. Chem. Phys. **86**, 1118 (1987).
[51] M. P. Casassa, Chem. Rev. (Washington, D.C.) **88**, 815 (1988).
[52] M. R. Nimlos, M. A. Young, E. R. Bernstein, and D. F. Kelley, J. Chem. Phys. **91**, 5268 (1989).
[53] R. Yamamoto, T. Ebata, and N. Mikami, J. Chem. Phys. **114**, 7866 (2001).
[54] A. V. Davis, R. Wester, A. E. Bragg, and D. M. Neumark, J. Chem. Phys. **117**, 4282 (2002).
[55] A. V. Davis, R. Wester, A. E. Bragg, and D. M. Neumark, J. Chem. Phys. **119**, 2020 (2003).
[56] R. S. Urdahl, K. D. Rector, D. J. Myers, P. H. Davis, and M. D. Fayer, J. Chem. Phys. **105**, 8973 (1996).
[57] R. S. Urdahl, D. J. Myers, K. D. Rector, P. H. Davis, B. J. Cherayil, and M. D. Fayer, J. Chem. Phys. **107**, 3747 (1997).
[58] D. Schwarzer, J. Troe, M. Votsmeier, and M. Zerezke, J. Chem. Phys. **105**, 3121 (1996).
[59] D. Schwarzer, J. Troe, and M. Zerezke, J. Chem. Phys. **107**, 8380 (1997).
[60] M. O. Hale, G. E. Galica, S. G. Glogover, and J. L. Kinsey, J. Phys. Chem. **90**, 4997 (1986).
[61] F. Markel and A. B. Myers, Chem. Phys. Lett. **167**, 175 (1990).
[62] The tunable infrared light comes from mixing the fundamental of an injection seeded Nd:YAG laser (Spectra Physics, LAB 170) with the output of a Nd:YAG pumped dye laser (Continuum, ND600) in a BBO crystal to produce the difference frequency.
[63] The fits yield maximum vibrational temperatures of 610 K in $CCl_4$, 350 K in $CDCl_3$, and 512 K in $(CD_3)_2CO$.
[64] G. C. G. Waschewsky, R. Horansky, and V. Vaida, J. Phys. Chem. **100**, 11559 (1996).
[65] D. J. Donaldson, V. Vaida, and R. Naaman, J. Chem. Phys. **87**, 2522 (1987).
[66] F. Ito and T. Nakanaga, J. Chem. Phys. **119**, 5527 (2003).
[67] A RRKM calculation for the dimer with 6000 $cm^{-1}$ of excess energy yields a dissociation time of 1.1 ps, based on the intra- and intermolecular vibrational frequencies of F. Ito, T. Nakanaga, Y. Futami, S. Kudoh, M. Takayanagi, and M. Nakata, Chem. Phys. Lett. **343**, 185 (2001).
[68] According to Ref. 64, the limiting values for the dimer fraction at 50 Torr are 15% and 51%, and at 373 K the limits are 19% and 66%.
[69] R. Pearman and M. Gruebele, J. Chem. Phys. **108**, 6561 (1998).
[70] M. Gruebele and R. Bigwood, Int. Rev. Phys. Chem. **17**, 91 (1998).
[71] M. Gruebele, Adv. Chem. Phys. **114**, 193 (2001).
[72] T. Shimanouchi, *Tables of Molecular Vibrational Frequencies* (National Bureau of Standards, Washington, D.C., 1972).